

BIO-INSPIRED FLUIDIC THERMAL ANGULAR ACCELEROMETER

Hommoood Alrowais¹, Patrick Getz¹, Min-gu Kim¹, Jin-Jyh Su^{1,2} and Oliver Brand¹

¹School of Electrical and Computer Engineering, Georgia Institute of Technology, Atlanta, USA

²Texas Instruments, Dallas, USA

ABSTRACT

This paper reports on a bio-inspired angular accelerometer based on a two-mask microfluidic process using a PDMS mold. The sensor is inspired by the semicircular canals in mammalian vestibular systems and pairs a fluid-filled microtorus with a thermal detection principle based on thermal convection. With inherent linear acceleration insensitivity, the sensor features a sensitivity of $29.8\mu\text{V}/\text{deg}/\text{s}^2=1.7\text{mV}/\text{rad}/\text{s}^2$, a dynamic range of $14,000\text{deg}/\text{s}^2$ and a detection limit of $\sim 20\text{deg}/\text{s}^2$.

INTRODUCTION

Miniaturized inertial sensors have been explored extensively over the past decade, and are used today in a wide variety of medical, consumer, defense and industrial applications [1,2]. This growth has been fueled by many design innovations resulting in device miniaturization, power consumption reduction, and sensitivity enhancements. On the other hand, nature -through natural selection- has evolved over thousands of years an elegant sensor design to sense rotational movement, and inherently reject linear motion [3]. In this paper, we propose a simplified bio-inspired angular accelerometer.

Inertial sensors have utilized various designs, such as suspended masses [4,5] and cantilevers [6], and transduction mechanisms, including capacitive [4], piezoresistive, [6] and thermal [7] transduction, to sense inertial inputs. Some of these structures do not inherently/passively cancel any linear cross-axis sensitivity, but utilize active measurements to remove the unwanted linear component of the motion signal [8]. Other devices use multiple sensors to distinguish linear and rotational input [9]. A design that eliminates the linear acceleration signals is a fluid-filled torus due to the fluid's motion in the opposing sides of the torus, impeding each other's motion [10].

The proposed design is based on the mammalian vestibular system's semicircular canal (SCC). The SCC is a rigid boney torus in the inner ear, intersected by a flexible membrane, filled with a water-like fluid [10]. Deflections in the membrane caused by an inertial input causes deflections in the hair cells embedded in the membrane. The stress induced in the hair cells sends a signal proportional to angular motion through the vestibular nerve to the brain.

The bio-inspired design presented here replaces the mechanical-to-electrical transduction by a thermal-to-electrical mechanism. Recently, thermal transduction has been used to sense linear motion [11]. These devices can sense motion along all three axes, with low power and high bandwidth. Previous attempts to implement thermal transduction along a fluid-filled torus relied on a complex

fabrication process [12]. In this work, we build on our previous design [13] and present a simplified, two-mask fabrication process.

With mammalian inertial sensors in mind, the sensor's target specifications include a dynamic range of $0-10,000\text{deg}/\text{sec}^2$, a frequency bandwidth of 20Hz, low cross-axis sensitivity and a low limit of detection of $1-2\text{deg}/\text{sec}^2$. This paper starts with the design principles behind the sensor, followed by the fabrication process, simulation and experimental results. It will conclude with some final remarks and future work.

DESIGN AND SIMULATION

Design

The design comprises four or more linear thermal accelerometers that are placed along the circumference of a microfabricated torus to detect the tangential acceleration along the torus (Figure 1). The tangential acceleration relates to the angular acceleration though $\alpha=a/R$, where α , a , and R are the angular acceleration, tangential acceleration, and major radius of the torus, respectively.

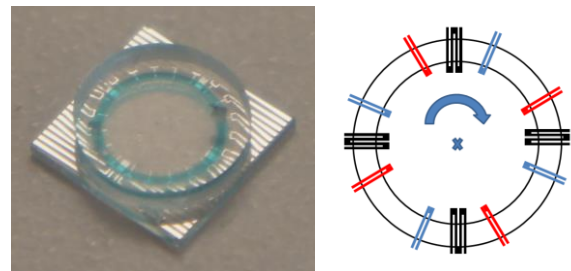


Figure 1: (Left) Optical image of angular accelerometer with microtorus radius $R=2.85\text{mm}$. (Right) Angular acceleration sensor schematic with heaters (black) and thermal sensors (red and blue) arranged along a half-torus; Upon clockwise angular acceleration, the red thermal sensors will experience an increase in temperature, while the blue ones see a temperature decrease.

The working principle behind the sensor is shown in Figure 1. A fluid-filled torus is formed on top of a set of heaters and temperature sensors. Each heating resistor has a pair of temperature sensors placed on either side. Multiple thermal sensors, comprising of a heating and two temperature-sensitive resistors, are placed along the circumference of the torus. A rotational inertial input will cause a change in the symmetrical temperature profile around the heater. This temperature asymmetry is detected by the temperature-sensitive resistors due to the temperature coefficient of their resistance. It should be noted that two effects contribute to the output signal in case of the thermal sensing: (1) the *inertial effect* due to

the inertia of the fluid in the microtorus and (2) the *buoyancy effect* due to density variations of the heated fluid.

Figure 1 shows an optical image of a fabricated angular accelerometer design with $R = 2.85\text{mm}$. Each meandering heater structure has a length and width of $750\mu\text{m}$ and $390\mu\text{m}$, respectively, while the temperatures sensor are $750\mu\text{m}$ long and $45\mu\text{m}$ wide. To simplify the fabrication and packaging process, a half-torus was used as the microfluidic channel. The heaters and sensors are fabricated on a glass substrate to minimize heat losses to the body of the device, and maximize heat transfer to the fluid. The simplicity of design and the lack of moving parts allow the device to be a shock resistant platform.

The main property of the fluid that impacts the device's performance is the fluid diffusivity [14], affecting both the frequency response and the sensitivity of the device. More diffusive fluids such as helium will have a higher bandwidth but a lower sensitivity. Less diffusive fluids such as CO_2 or liquids will have higher sensitivity, but smaller bandwidth. The cut-off frequency is proportional to $\sim\chi/r^2$, where χ is the gas diffusivity, and r is the minor radius of the channel [14]. The increase in sensitivity is offset by a reduction in bandwidth. This can be overcome by operating the device in a closed loop configuration with a PID controller. [15]

The fluid chosen for the present structure is a silicone oil (Sigma Aldrich), because of its low-vapor pressure (less than $1\mu\text{Torr}$), relatively high thermal conductivity (0.1W/mK), and low viscosity (5cSt). Aluminum was chosen as resistor material for its high temperature coefficient of resistance (3900ppm/K). An aluminum alloy with 3% copper was used in the final structure to minimize the effect of electromigration [16].

Finite Element Analysis

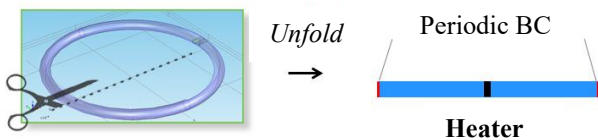


Figure 2: Simplifying the 3D torus structure into a linear pipe with periodic boundary conditions for computational purposes.

A finite element analysis of the sensor was performed using COMSOL 5.1 (Burlington, MA). The simulation process started with a simplified linear channel with symmetric boundary conditions, as shown in Figure 2. This was followed by a 3D simulation of the full structure. The simplified model was used to optimize the design of the structure due to its fast simulation times. A body force was applied to the fluid to simulate the applied angular acceleration. A constant power was applied to the heating resistor. As an example, Figure 3 shows the simulated step response of the structure, i.e. the maximum flow velocity of the fluid in the center of the torus, to a 1deg/s^2 input. Figure 4 shows the simulated temperature

profile around the heating resistor, which was used for the optimal placement of the temperature sensors.

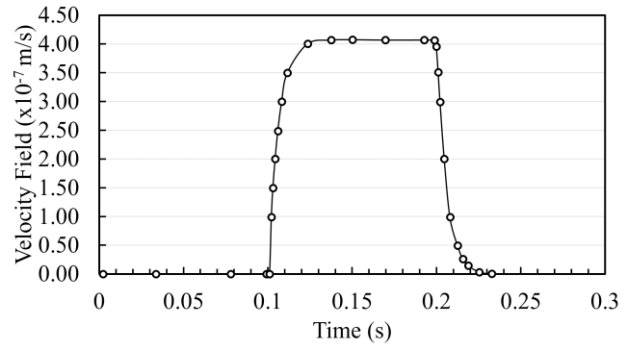


Figure 3: Simulated step-response of the angular accelerometer, i.e., maximum flow velocity in the center of the microtorus as a function of time, for a 0.1sec pulse with 1deg/s^2 angular acceleration. The measured time constant of 4ms corresponds to a sensor cut-off of 40Hz .

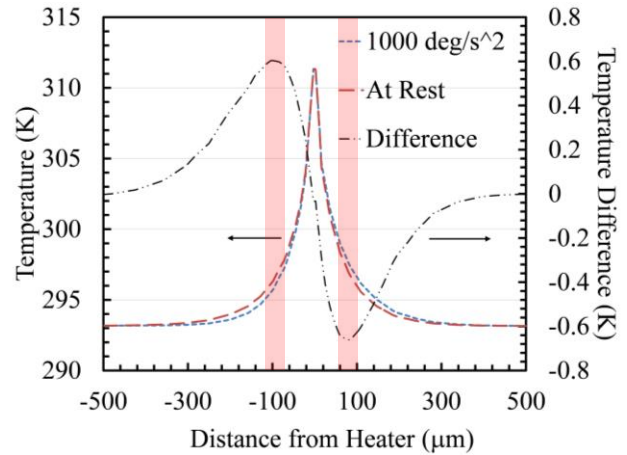


Figure 4: Simulated temperature profile along torus (left and right of a heater) for $\alpha=0$ and 1000deg/s^2 as well as temperature difference between both profiles, showing the optimal location of the temperature sensors highlighted in red.

FABRICATION

The fabrication process (see Figure 5) starts with depositing 125nm of aluminum via sputtering on a glass wafer. The aluminum resistors are patterned and etched using reactive ion etching. To create the microfluidic channel, an inverse mold of the structure is built using CNC milling (HAAS) as described in [17]. PDMS is cast on the aluminum. After crosslinking the PDMS in a 50 degree oven for 1 hour, two inlet holes are punctured into the microfluidic channel. The PDMS cover and glass substrate are bonded after exposing them to an oxygen plasma for 1 minute ($< 200\text{mTorr}$, 18W). The bonded device is wire bonded to a 28 -pin ceramic package to ease electrical connection. The structure is filled with fluid using a vacuum process [18]. Finally, the packaged device is covered with UV-enabled epoxy EPO-TEK OG116 (Epoxy Technologies, MA, USA) and exposed to a broadband UV light source for thirty minutes.

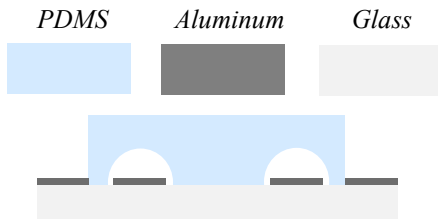


Figure 5: Cross-section of packaged sensor with glass substrate with patterned metal resistors and bonded PDMS mold with imprinted microchannel.

EXPERIMENTAL RESULTS

Figure 6 shows a thermal IR image (FLIR A315) of the device with heating power applied to the heater. The maximum temperature rise detected for a heating power of 10mW was 15 degrees.

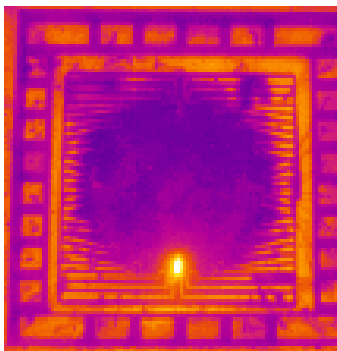


Figure 6: Thermal IR image of uncovered sensor. The bright spot shows a heater with 10mW heating power applied, resulting in a 15°C temperature increase.

The sensor output was measured as shown in Figure 7. The temperature sensors R+ and R- are connected in a Wheatstone bridge configuration. The Wheatstone bridge output signal is amplified using an instrumentation amplifier (TI INA551), and then passed through a passive low-pass filter to eliminate high-frequency noise. The output is displayed on an oscilloscope (Tektronix TDS2022C) for direct viewing and also connected to a lock-in amplifier (Stanford Research Systems 830) for recording the signal amplitude.

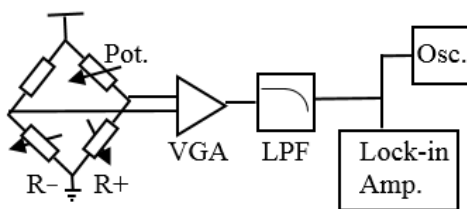


Figure 7: Interface circuitry and experimental setup for measurement of the output bridge voltage.

Rotational motion is applied by connecting the sensor to a stepper motor (SureStep 23079), which was controlled using analog input from a function generator (Tektronix AFG3022B) to induce rotational motion.

Linear acceleration was applied using a linear stage (Rockwell Automation MPAS-A6066B).

The device's output to a 4Hz sinusoidal angular acceleration is presented in Figure 8. The resulting output signal is linear with the applied angular acceleration with a sensitivity of 29.8μV/(deg/s²), and the smallest detectable angular acceleration was 20deg/s². The frequency behavior of the structure under 5000deg/s² angular acceleration is shown Figure 9, showing the low cut off frequency due to the used silicone oil.

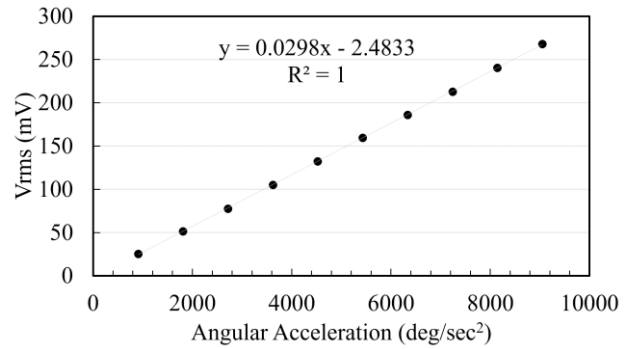


Figure 8: Amplified signal output voltage as a function of the angular acceleration applied ($f=4\text{Hz}$). The sensitivity is 29.8μV/(deg/s²)=1.7mV/rad/s²; the lowest detectable angular acceleration was 20deg/s².

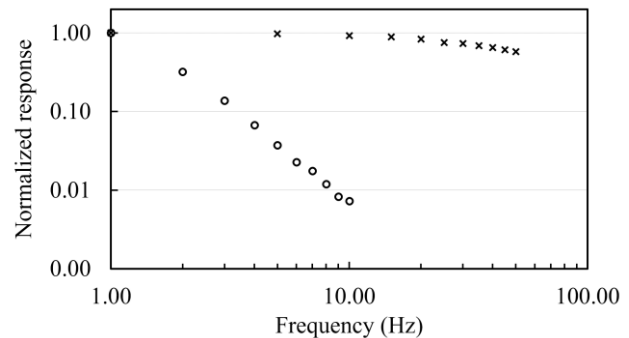


Figure 9: Simulated (x) and measured (o) frequency transfer characteristic. An angular acceleration of ~5000deg/s² was applied. The simulated and measured responses were normalized to their low frequency values for better comparison. The tested device has a channel radius of 400μm.

The device's cross-axis sensitivity to linear acceleration is shown in Figure 10. The device's sensitivity to the equivalent linear acceleration of rotational motion is twenty times higher in magnitude than the signal generated by an applied linear acceleration. The remaining cross-sensitivity can be further reduced by analyzing the response of multiple sensors arranged along a single microtorus (see Figure 1). A bubble inside the microtorus breaks the symmetry of the design and, thus, results in a higher sensitivity to linear acceleration (see Figure 10). Table 1 summarizes the characteristics of a sample device.

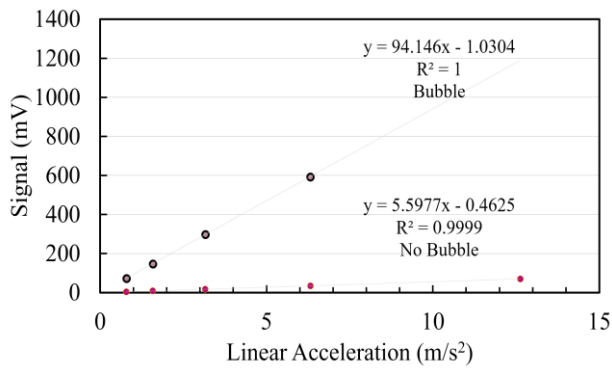


Figure 10: Cross-sensitivity to applied linear acceleration for two cases: (i) completely fluid-filled microtorus (no bubble) and (ii) fluid-filled microtorus with small bubble.

Table 1: Summary of a sample device characteristics.

Major Radius	2.85mm
Minor Radius	400 μ m
Heater Resistance	500 Ω
Temperature Sensor Resistance	200 Ω
Bandwidth	4Hz
Fluid	Silicone Oil (5cSt)
Dynamic Range	0-14,000deg/s ²
Limit of detection	\sim 20deg/s ²

CONCLUSION

The demonstrated bio-inspired angular accelerometer combines high sensitivity, linear acceleration rejection and low bandwidth with a simplified fabrication process. The device's power consumption can be improved by pulse-operating the device.

ACKNOWLEDGEMENTS

This work was supported in part by the Saudi Arabian Ministry of Education. The authors would like to thank Georgia Tech IEN cleanroom staff for fabrication support, and Dr. Degertekin for using his lab facilities.

REFERENCES

- [1] K. Liu, W. Zhang, W. Chen, K. Li, F. Dai, F. Cui, X. Wu, G. Ma, and Q. Xiao, "The development of micro-gyroscope technology," *J. Micromech. Microeng.*, vol. 19, no. 11, p. 113001, 2009.
- [2] N. Yazdi, F. Ayazi, and K. Najafi, "Micromachined Inertial Sensors," *Proceedings of the IEEE*, vol. 86, pp. 1640–1659, 1998.
- [3] G. H. Crampton, "Does Linear Acceleration Modify Cupular Deflection?," *NASA Special Publication*, vol. 115, p. 169, 1966.
- [4] G.J. O'Brien, D.J. Monk, and K. Najafi. "Angular Accelerometer with Dual Anchor Support," in *Proc. Transducers 2003 Conference*, pp. 1371–1374, 2003.
- [5] T.J. Brosnihan, A. Pisano, and R. Howe, "Surface Micromachined Angular Accelerometer with Force Feedback," in *Digest ASME International Conference and Expo*, pp. 941–947, 1995.
- [6] Furukawa, Naoyuki, and K. Ohnishi, "A Structure of Angular Acceleration Sensor Using Silicon Cantilevered

Beam with Piezoresistors," in *Industrial Electronics, Control, Instrumentation, and Automation*, pp.1524–1529, 1992.

[7] A.M. Leung, J. Jones, E. Czyzewska, J. Chen, and B. Woods, "Micromachined Accelerometer based on Convection Heat Transfer," in *Proc. IEEE MEMS Conference*, pp. 627–630, 1998.

[8] E.J. Eklund, and A.M. Shkel. "Single-mask SOI Fabrication Process for Linear and Angular Piezoresistive Accelerometers with On-chip Reference Resistors," in *IEEE Sensors*, pp. 4, 2005.

[9] R. Amarasinghe, D.V. Dao, T. Toriyama, and S. Sugiyama, "Design and Fabrication of Miniaturized Six-Degree of Freedom Piezoresistive Accelerometer," in *IEEE MEMS Conference*, pp. 351–354, 2005.

[10] V. J. Wilson, J. Buttner-Ennever, and K. E. Cullen, *The Vestibular System: A Sixth Sense*, Oxford University Press, pp. 78–82, 2012.

[11] Wang, S.S.; Gong, X.H.; Nie, B.; Yuan, W.Z.; Chang, H.L., "A micromachined fluidic reduced inertial measurement unit using thermal expansion flow principle," in *Proc. Transducers 2015 Conference*, pp. 1223–1226, 2015.

[12] J. Groenesteijn, H. Droogendijk, M.J. de Boer, R.G.P. Sanders, R.J. Wiegerink, and G.J.M. Krijnen, "An Angular Acceleration Sensor Inspired by the Vestibular System with a Fully Circular Fluid-channel and Thermal Read-out," in *IEEE MEMS Conference*, pp. 696–699, 2014.

[13] H. Alrowais, O Brand, and P Bhatti, "Design, Simulation and Fabrication of Thermal Angular Accelerometer," in *Proc. Hilton Head Workshop on Solid-State Sensors, Actuators, and Microsystems*, pp. 243–246, 2014.

[14] J. Courteaud, N. Crespy, P. Combette, B. Sorli, and A. Giani, "Studies and Optimization of the Frequency Response of a Micromachined Thermal Accelerometer," in *Sensors and Actuators A: Physical*, vol. 147, pp. 75–82, 2008.

[15] A. Garraud, P. Combette, A. Deblonde, P. Loisel, and A. Giani, "Closed-loop micromachined accelerometer based on thermal convection," *IET Micro Nano Letters*, vol. 7, pp. 1092–1093, 2012.

[16] A. J. Learn, "Electromigration effects in aluminum alloy metallization," in *Journal of Electronic Materials*, vol. 3, pp. 531–552, 1974.

[17] M. E. Wilson, N. Kota, Y. Kim, Y. Wang, D. B. Stolz, P. R. LeDuc, and O. B. Ozdoganlar, "Fabrication of circular microfluidic channels by combining mechanical micromilling and soft lithography," in *Lab Chip*, vol. 11 pp. 1550–1555, 2011.

[18] J. Monahan, A. A. Gewirth, and R. G. Nuzzo, "A method for filling complex polymeric microfluidic devices and arrays," in *Anal. Chem.*, pp. 3193–3197, 2001.

CONTACT

* H. Alrowais, School of Electrical and Computer Eng., Georgia Institute of Technology, 777 Atlantic Drive NW, Atlanta, Georgia 30318, USA; Tel: +1-404-809-5463; E-mail: hommood.alrowais@gatech.edu.